www.czasopisma.pan.pl PAN POLSKA AKADEMIA NAUK www.journals.pan.pl

PAN ARCHIVES OF ACOUSTICS
Vol. **43**, No. 3, pp. 517–529 (2018)

DOI: 10.24425/123923

Technical Notes

Acoustical Assessment of Automotive Mufflers Using FEM, Neural Networks, and a Genetic Algorithm

Ying-Chun CHANG[(1)], Min-Chie CHIU[(2)], Meng-Ru WU[(1)]

[(1)] *Department of Mechanical Engineering*
Tatung University
Taiwan, ROC

[(2)] *Department of Mechanical and Automation Engineering*
Chung Chou University of Science and Technology
6, Lane 2, Sec.3, Shanchiao Rd., Yuanlin, Changhua 51003, Taiwan, R.O.C.;
e-mail: minchie.chiu@msa.hinet.net

(*received May 31, 2017; accepted February 28, 2018*)

In order to enhance the acoustical performance of a traditional straight-path automobile muffler, a multi-chamber muffler having reverse paths is presented. Here, the muffler is composed of two internally parallel/extended tubes and one internally extended outlet. In addition, to prevent noise transmission from the muffler's casing, the muffler's shell is also lined with sound absorbing material.

Because the geometry of an automotive muffler is complicated, using an analytic method to predict a muffler's acoustical performance is difficult; therefore, COMSOL, a finite element analysis software, is adopted to estimate the automotive muffler's sound transmission loss. However, optimizing the shape of a complicated muffler using an optimizer linked to the Finite Element Method (FEM) is time-consuming. Therefore, in order to facilitate the muffler's optimization, a simplified mathematical model used as an objective function (or fitness function) during the optimization process is presented. Here, the objective function can be established by using Artificial Neural Networks (ANNs) in conjunction with the muffler's design parameters and related TLs (simulated by FEM). With this, the muffler's optimization can proceed by linking the objective function to an optimizer, a Genetic Algorithm (GA).

Consequently, the discharged muffler which is optimally shaped will improve the automotive exhaust noise.

Keywords: acoustics; finite element method; genetic algorithm; muffler optimization; polynomial neural network model.

Notations

This paper is constructed on the basis of the following notations:

B_0, B_i, B_{ij}, B_{ijk} – the coefficient of the node function in the ANN,
CPM – the product of the penalty function,
FSE – the deviation of mean square,
m – the number of the design parameters,
N – the number of training data,
NN_p – the total possible searching number ($= 2^m$),
N_i – the i-th parameters of the polynomial neural network,
Q – he number of the network's coefficients,
x_i, x_j, x_k – the input data in the ANN,
y_k – the output value in the ANN,
K_i – the geometric factor of the pressure drop for the i-th intersection of the duct,
k_p – the penalty function in the ANN,
$\widehat{y}_i$ – the required data in the ANN,
y_i – the predicted data for the ANN,
σp^2 – the error variation in the ANN,
D – the diameter of the first chamber's inlet duct [m],
bit – bit length of chromosome,
$iter_{\max}$ – maximum iteration during GA optimization,
L – the length of the extended duct in the second chamber [m],
L_1 – the length of the extended duct in the first chamber [m],
L_{in} – the length of the second chamber's inlet duct [m],
pc – crossover ratio,
pm – mutation ratio,
pop – number of population,
TL – transmission loss [dB].

1. Introduction

Research on simply shaped mufflers has been examined using theoretical derivations (Chang *et al.*, 2004; Yeh *et al.*, 2006). However, because of the complicated geometry of commercial automobile mufflers, an acoustical assessment using a theoretical analysis is not accessible.

In 1994, Mo and Huh (1994) predicted the acoustic transmission loss of a muffler using NASTRAN, a FEM (Finite Element Method) package. Panigrahi and Munjal (2007) analyzed a perforated cross-flow reactive muffler with CFD (Computational fluid dynamics). Later, a branch of fluid mechanics used numerical analysis and algorithms to solve and analyze problems that involved fluid flows. Mohiuddin *et al.* (2007) analyzed the acoustical performance of a reactive muffler using FLUENT software. Fang *et al.* (2009) assessed the flow field and the total pressure distribution inside a muffler using the CFD method. Chen and Shi (2011) investigated the influence of the internal flow on the performance of a muffler via Fluent modeling. Kore *et al.* (2011) simulated the flow field and the transmission loss of a reactive muffler using Fluent. Vasile and Gillich (2012) estimated the transmission loss of a combustion engine with COMSOL. Reddy *et al.* (2012) developed reactive mufflers using NASTRAN Software. Rajadurai and Ananth (2014) designed reactive mufflers using CATIA Software. Tajane *et al.* (2014) investigated automobile exhaust systems using ANSYS Software. Galphade and Patil (2015) assessed a car's muffler using CFD Software. Somashekar *et al.* (2015) analyzed automobile mufflers using NASTRAN Software. However, the optimization of the muffler's shape in the above research has been routinely neglected. To reach optimization, Chang *et al.* (2009) and Chiu and Chang (2009) developed an optimization method for a muffler that had a simple geometrical shape by using a neural network and a genetic algorithm. Based on the analytic method, Chiu (2013) also accessed optimal multi-chamber mufflers hybridized with extended tubes in a series. Nevertheless, the muffler's geometry was simple.

There have been many kinds of commercialized automotive mufflers developed in the past decade. The acoustical elements of a resonating tube and a straight perforated tube have been widely used. However, its acoustical performance is reduced as the noise wave propagates via a straight venting path. In order to enhance the acoustical performance, a multi-chamber muffler with a reverse path that increases noise reduction is introduced. Here, a complex-shaped muffler hybridized with two internally parallel/extended tubes and one internally extended outlet is suggested. In addition, to prevent noise transmission from the muffler's casing, the muffler's shell is lined with sound absorbing material. To facilitate muffler optimization, a simplified mathematical model that serves as an objective (OBJ) function (or fitness function) linking the optimizer is presented. Moreover, the objective function is built by using Artificial Neural Networks (ANNs) in conjunction with input data (the muffler's design parameters) and output data (a related TL calculated by FEM). Additionally, a genetic algorithm (GA) is adopted as the optimizer.

2. Mathematical Model of the FEM (Run on the COMSOL Package)

An automotive muffler composed of several extended tubes, an internally partitioned baffle, and an internal sound absorbing material covered with a perforated plate is presented and shown in Fig. 1. The boundary condition for the acoustical field of the non-perforated tube (a solid boundary) used in the acoustical model with the COMSOL package is

$$n \cdot \left\{ \frac{1}{\rho_c}(\nabla p_t - q) \right\} = 0, \tag{1}$$

where q (a dipole sound source) is set at zero, c (the sound speed) is set at 343 m/s, and ρ (air density) is set at 1.293 kg/m^3.

The boundary condition for the acoustical field of the perforated tube (a solid boundary) used in the acoustical model is

$$n \cdot \left\{ \frac{1}{\rho_c}(\nabla p_t - q) \right\} = -(p_{t1} - p_{t2}) \frac{i\omega}{Z_i}, \tag{2}$$

$$Z_i = \rho_c c_c \left[\frac{1}{\sigma} \sqrt{\frac{8\mu k}{\rho_c c_c}} \left(1 + \frac{t_p}{d_h} \right) + \theta_f + i \frac{k}{\sigma} (t_p + \delta_h) \right], \tag{3}$$

where t_p is the thickness of the perforated tube, d_h is the diameter of the perforated hole, σ is the perforated rate of the perforated tube, μ is the dynamic viscosity of the air, θ_f is the flowing resistance, and δ_h is the end correction factor; μ is set at $1.8 \cdot 10^{-5}$ Pa·s.

The governing equation of the sound wave propagating into the muffler yields

$$\nabla \cdot -\frac{1}{\rho_c}(\nabla p_t - q) - \frac{k_{eq}^2 p_t}{\rho_c} = Q, \tag{4}$$

where

$$p_t = p + p_b, \qquad k_{eq}^2 = \left(\frac{\omega}{c_c} \right)^2,$$

$$c_c = c, \qquad \rho_c = \rho.$$

Here, p_b is the background pressure field.

The Sound Transmission Loss (TL) is calculated as

$$\mathrm{TL} = 10 \log \frac{W_{\mathrm{in}}}{W_{\mathrm{out}}}, \tag{5}$$

where W_{in} is the inlet sound power, W_{out} is the outlet sound power, and W_0 is the referred sound power.

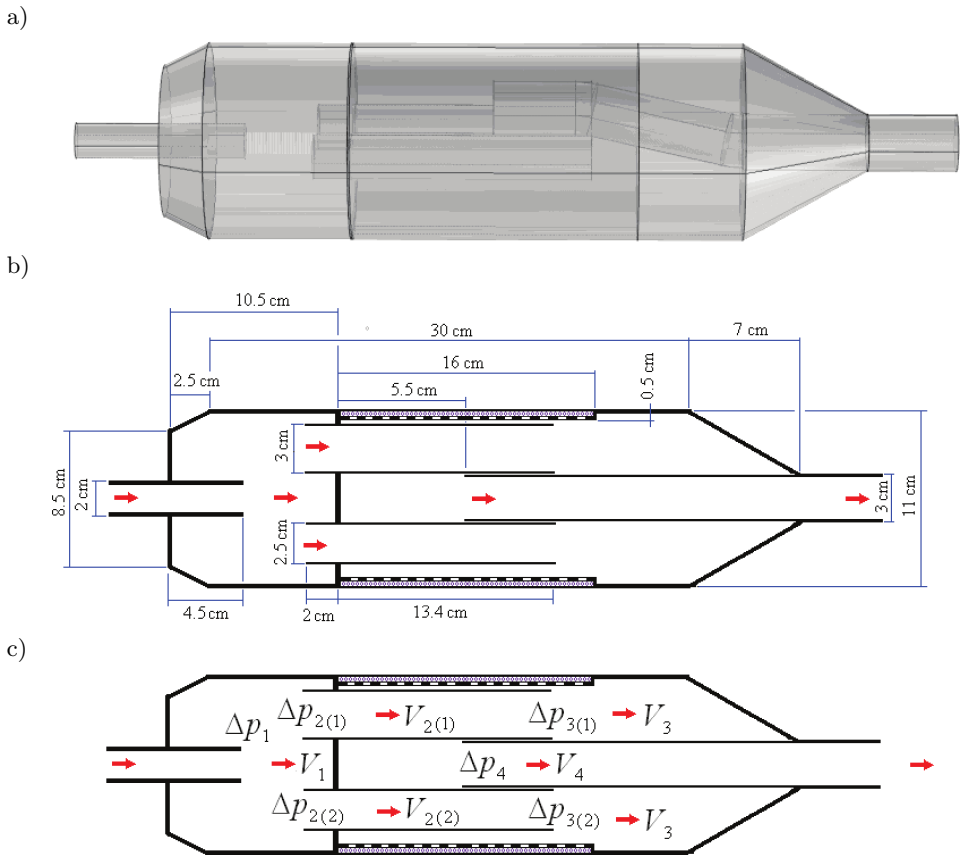

Fig. 1. Mechanism of an automotive muffler: a) prototype of the automotive muffler, b) dimension of the automotive muffler, c) pressure drops of the automotive muffler.

According to Bie *et al.* (1988), the mean pressure drop (Δp_T) of the mufflers with extended tubes is

$$\begin{aligned}\Delta p_T &= \Delta p_1 + \Delta p_{2(1)} + \Delta p_{2(2)} + \Delta p_{3(1)} + \Delta p_{3(2)} \\ &\quad + \Delta p_4 = K_1 \cdot \rho V_1^2/2 + K_{2(1)} \cdot \rho V_{2(1)}^2/2 \\ &\quad + K_{2(2)} \cdot \rho V_{2(2)}^2/2 + K_{3(1)} \cdot \rho V_{3(1)}^2/2 \\ &\quad + K_{3(2)} \cdot \rho V_3^2/2 + K_4 \cdot \rho V_4^2/2, \qquad (6)\end{aligned}$$

$$\begin{aligned} K_1 &\fallingdotseq 1.0; & K_{2(1)} &= 1.0; \\ K_{2(2)} &= 1.0; & K_{3(1)} &= 1.0; \\ K_{3(2)} &= 1.0; & K_4 &\fallingdotseq 1.0, \end{aligned}$$

where K_i is the geometric factor of the pressure drop for the i-th intersection of the duct.

2.1. Model check

The automotive muffler shown in Fig. 1 is composed of several extended tubes, an internally partitioned baffle, and an internal sound absorbing material covered with a perforated plate. Before performing an acoustical simulation on an automotive muffler, an accuracy check of the FEM mathematical model on the fundamental elements (a straight expansion chamber with an internally extended tube (shown in Fig. 2), internally partitioned baffle (shown in Fig. 3), and an

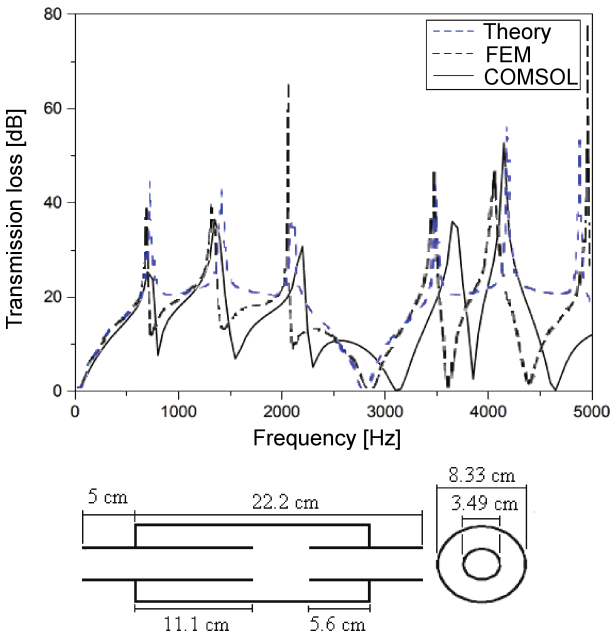

Fig. 2. Accuracy check of an internal straight tube-extended expansion chamber as compared to Lyu's theory (Lyu, 2005), FEM (Lyu, 2005), and COMSOL.

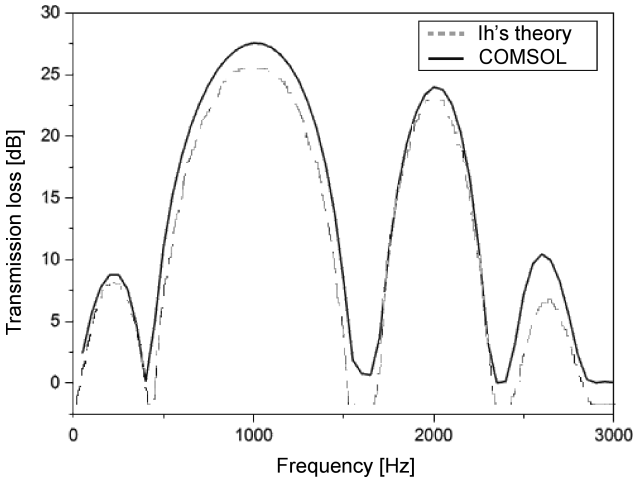

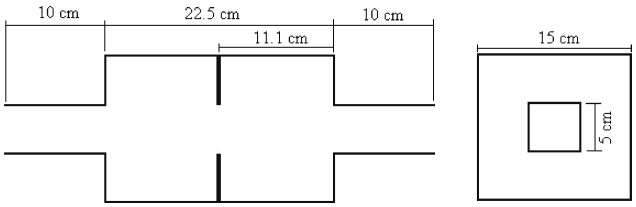

Fig. 3. Accuracy check of an internally partitioned baffle chamber as compared to Ih's theory (Ih, 1992) and COMSOL.

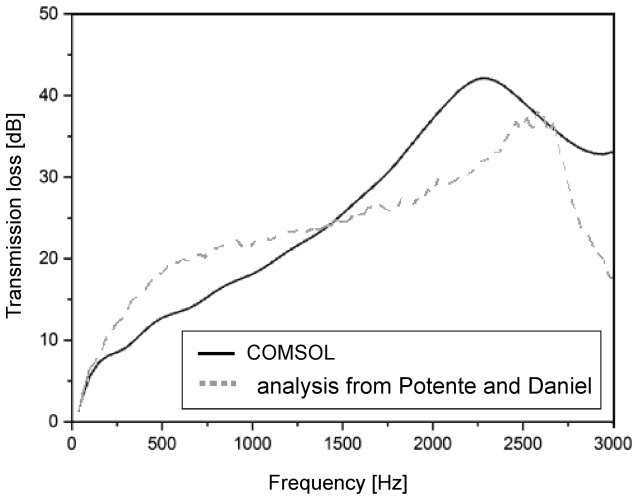

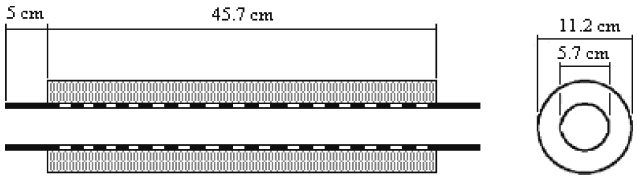

Fig. 4. Accuracy check of an internal sound absorbing material covered with a perforated plate as compared to Potente & Daniel's theory (Potente, Daniel, 2005) and COMSOL.

internally lined sound absorbing material covered with a perforated plate (shown in Fig. 4)) is performed using analytical data from (Lyu, 2005; Ih, 1992), and (Potente, Daniel, 2005). As illustrated in Figs. 2 and 3, both the FEM and the analytical data for the muffler are in agreement. For Fig. 4, the difference between the two curves is obvious. This might be because the parameter setting of wool's acoustical impedance with respect to FEM model and the analytical model is different; however, the tendencies of the profiles are roughly in agreement. Consequently, the simulation and optimization for the automotive muffler within a fixed space are carried out in the following section.

3. Sensitivity analysis

In order to investigate the sensitivity of the design parameters, the adjustments of the parameters are shown in Fig. 5. The acoustical performances with respect to frequencies using FEM are shown in Figs. 6–9. Results in Fig. 6 reveal that the profiles of the TL will be closely related to the length of L (the extended length of the second chamber in the muffler). Similarly, as indicated in Fig. 7, the TL curve will increase when the length of L_1 (the extended length of the first chamber in the muffler) increases. In addition, Fig. 8 indicates that the profiles of the TL will increase if the length of D (the diameter of the inlet for the first

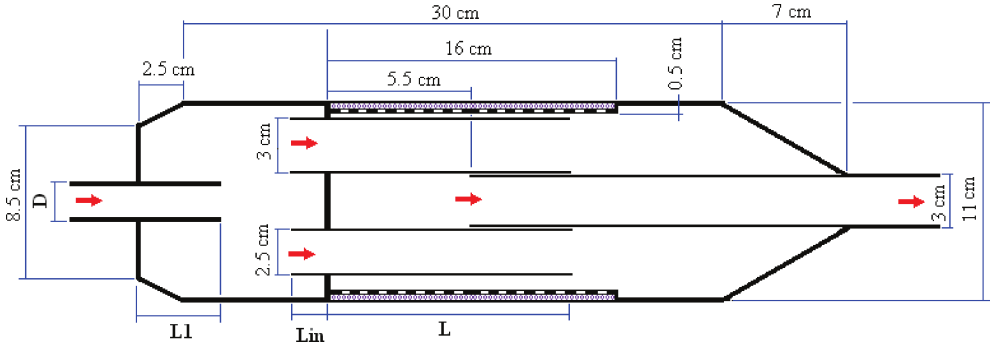

Fig. 5. The design parameters of an automotive muffler.

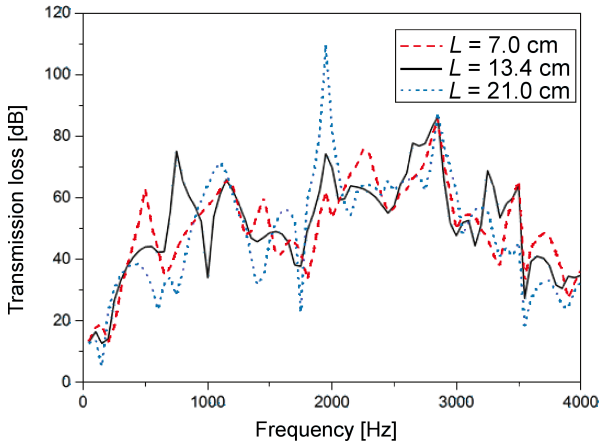

Fig. 6. TL profiles with respect to various values of parameter L.

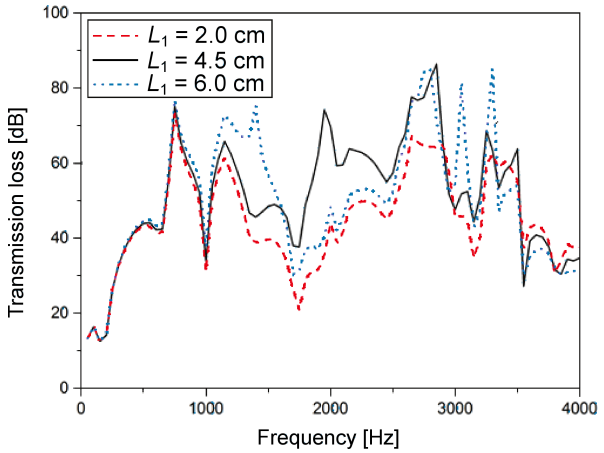

Fig. 7. TL profiles with respect to various values of parameter L_1.

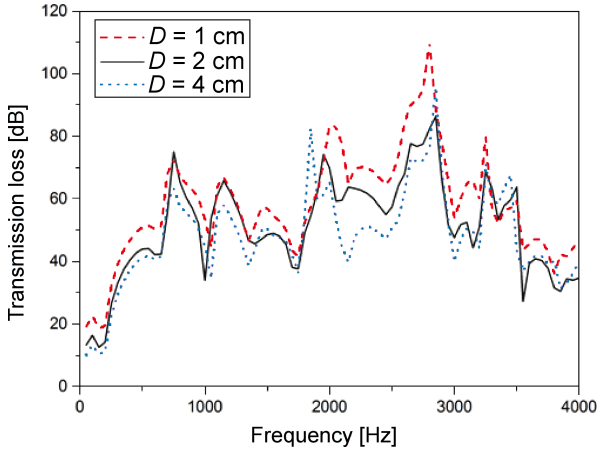

Fig. 8. TL profiles with respect to various values of parameter D.

chamber of the muffler) decreases. Moreover, as can be seen in Fig. 9, the profiles of the TL will also be closely related to the length of L_{in} (the inlet length of the second chamber in the muffler).

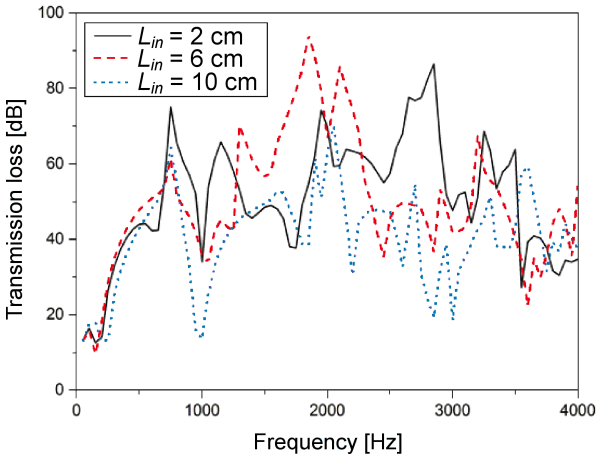

Fig. 9. TL profiles with respect to various values of parameter X.

Because the tendency for TL with respect to the other three parameters (L, L_1, and L_{in}) is close but uncertain, these design parameters (L, L_1, and L_{in}) are then selected as the design parameters during the optimization process.

4. Artificial Neural Network (ANN) Model

The ANN may be used as universal approximators; but the dependencies are implicit and hidden within the neural network structure. To overcome this inconvenience, an explicit function of a polynomial neural network is considered. Here, the polynomial neural network developed by Ivakhnenko (1971) is one kind of predictor for fish populations in rivers. With this, the interconnections between the layers of neurons can be simplified, and then an automatic algorithm for the structure design and weight adjustment can be established. On the basis of the GMDH (Group Method of Data Handling) feed-forward networks and short-term polynomial transfer functions, the coefficients of the polynomial transfer functions can be obtained via a regression process. The regression process will be combined by emulating the self-organizing activity which guides the artificial neural network's (ANN) structural learning. The polynomial neural network shown in Fig. 10 includes an input layer, a hidden layer, Σ (summation), and an output layer (product). Here, the hidden layer is the product of the input and weighted value (Patrikar, Provence, 1996). z_{jk}, the j-th output is

$$z_{jk} = \sum_{i=0}^{n} W_{ij} X_{ij}. \tag{7}$$

The total output of the neural network yields

$$y_k = \prod_{j=1}^{h} z_{jk}, \tag{8}$$

where h is the unit's number in a hidden layer.

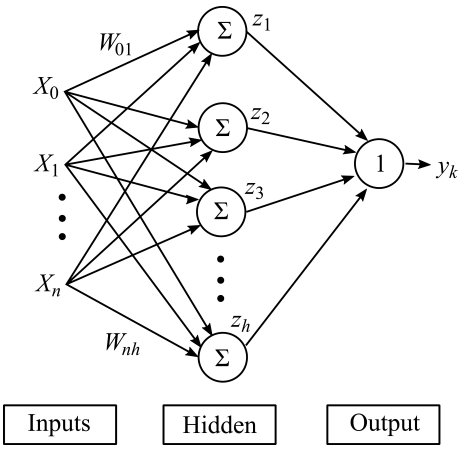

Fig. 10. Structure of an artificial neural network.

Plugging Eq. (7) into (8) yields

$$y_k = B_0 + \sum_{i=1}^{n} B_i x_i + \sum_{i=1}^{n}\sum_{j=1}^{n} B_{ij} x_i x_j + \sum_{i=1}^{n}\sum_{j=1}^{n}\sum_{k=1}^{n} B_{ijk} x_i x_j x_k + \ldots, \tag{9}$$

where y_k is the output value, x_i, x_j, x_k are the input data, and B_0, B_i, B_{ij}, and B_{ijk} are the coefficients of the node function.

Two kinds of acoustical optimizations (case I and case II) shown in Figs. 11 and 12 are exemplified.

Using the muffler's design parameters (case I: L_1 and L_{in}; case II: L_1 and L) as the input data and theo-

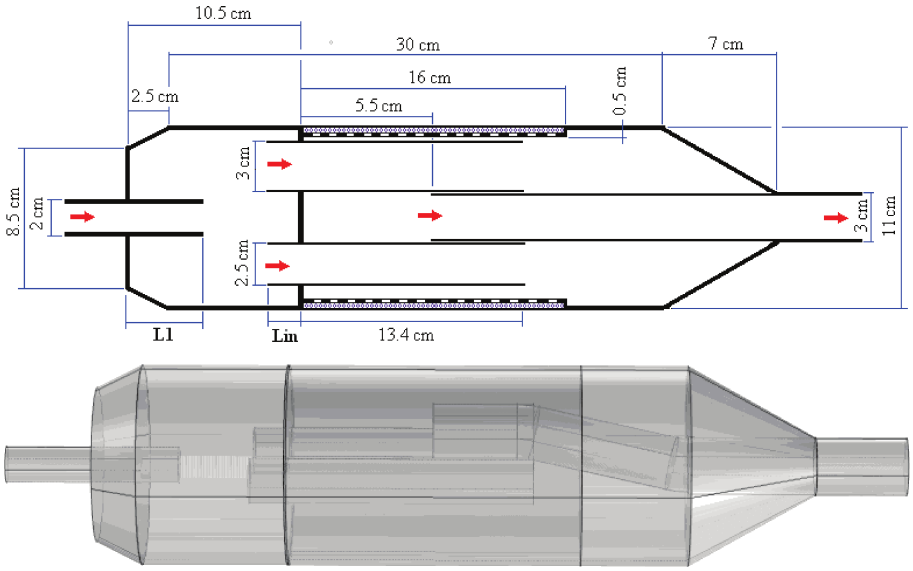

Fig. 11. Acoustical optimization in case I.

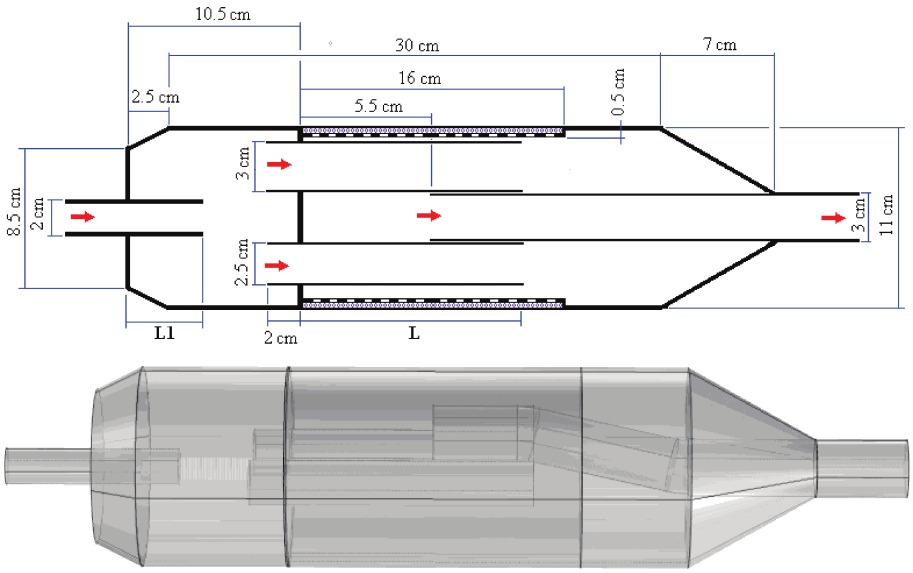

Fig. 12. Acoustical optimization in case II.

retical TL (simulated by the FEM) as the output data (TL) in the proposed ANN model (the fitness function or the objective function), a trained ANN model can be achieved using both the training data bank and the polynomial calculation in conjunction with the PSE standard (deviation of mean square) where PSE is in form of

$$\mathrm{PSE} = \mathrm{FSE} + k_p, \tag{10}$$

$$\mathrm{FSE} = \frac{1}{N}\sum_{i=1}^{N}(\widehat{y}_i - y_i)^2, \tag{11}$$

$$k_p = \mathrm{CPM}\frac{2\sigma p^2 Q}{N}. \tag{12}$$

Here, FSE is the deviation of the mean square, k_p is the penalty function, N is the number of training data, $\widehat{y}_i$ is the required data, y_i is the predicted data for the ANN model, CPM is the product of the penalty function, σp^2 is the error variation, and Q is the number of the network coefficients.

The flow diagram of the ANN model is depicted in Fig. 13. The predicted TL can be obtained by inputting arbitrary design data into the ANN model, a simplified OBJ function. With this, the optimal process of the mufflers can be performed by using the ANN model and the GA method.

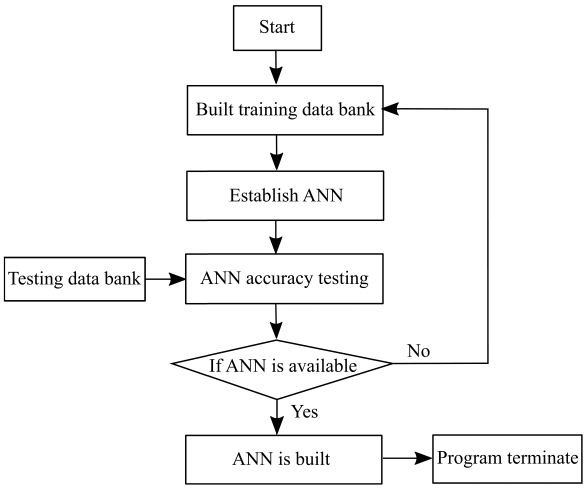

Fig. 13. Steps in the ANN model.

5. Genetic Algorithm

Holland (1975) first formalized Genetic Algorithms (GA) and later Jong (1975) developed and applied them in functional optimization. Based on the concept of Darwinian natural selection, GA's search strategies involve population size, selection strategy, mutation ratio, crossover ratio, maximum iteration, parameter numbers, length of the chromosome, the gene population, and the searching range of the parameters. Each new candidate's parent will be chosen by the coding/decoding transformation and the fitness (i.e., objective function) calculation. The precision [m] of the parameter search is

$$M = \frac{P_{\max} - P_{\min}}{NN_p - 1}, \tag{13}$$

where NN_p $(= 2^m)$ is the total possible searching number, m is the number of the design parameters, $P_{\max}$ is the maximum range of the parameter, and $P_{\min}$ is the minimum range of the parameter. The tournament selection is adopted as the elitism mechanism in the GA optimization. In addition, the uniform crossover is used in the optimization process. In order to generate a better offspring, the variety of chromosomes will be widened via a mutation scheme. The GA operations are illustrated in Fig. 14. Here, the process was terminated when the number of generations reached a pre-selected $iter_{\max}$.

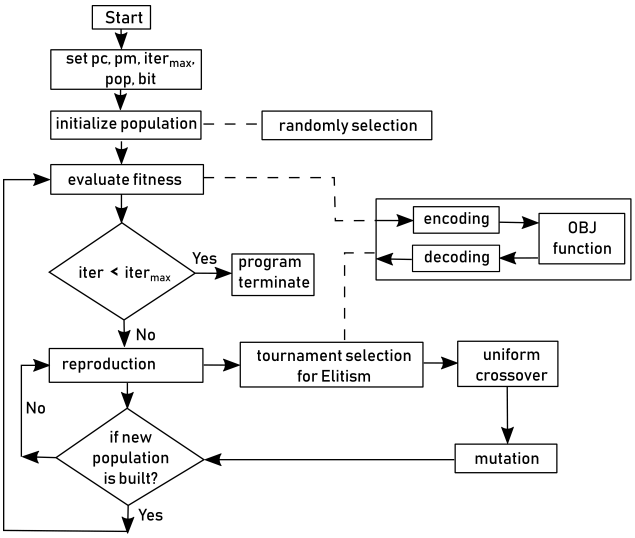

Fig. 14. GA optimization flow diagram.

6. Case study

A diesel engine with a power rate of 150 HP and a venting volume of 2000 cm^3 per cycle has a venting flow rate (Q) of 0.08325 m^3/s (Chiu *et al.*, 2016). According to Bie *et al.* (1988), the overall sound power level (SWL) emitted from a diesel engine at the exhaust outlet tube calculated by Eq. (14) is 128.7 dB(A)

$$SWL = 120 + 10\log_{10} kw - (lex/1.2), \tag{14}$$

where kw (kilo watt) is the diesel engine's power rate and l_{ex} $(= 0.3$ M) is the length of the exhaust outlet tube. Two primary peaks of the diesel engine's venting noise at 1000 Hz and 3000 Hz are found; therefore, two kinds of acoustical optimization (case I in Fig. 11 and case II in Fig. 12) are considered for reducing the targeted tones of 1000 Hz and 3000 Hz, respectively. To assure the existing back pressure of the muffler,

the diameters of the internal tubes will be fixed during the optimization process. As indicated in Fig. 11 (case I), two design parameters (L_1 and L_{in}) are chosen, where L_1 is the length of the extended inlet tube inside the first chamber and L_{in} is the length of the inlet for the second chamber. Similarly, as indicated in Fig. 12 (case II), L_1 and L are chosen as the optimization parameters. Here, L is the length of the extended inlet tube inside the first chamber.

6.1. Case I

To optimize the acoustical performance within a limited space, two kinds of design parameters – L_1 and L_{in} – are chosen as the tuned variables. The range and schedule levels of the parameters are depicted in Table 1. Therefore, using the FEM run on the COMSOL package, the TL with respect to sixteen training data sets shown in Table 2 is calculated. Taking L_1 and L_{in} as the input data and the resulting TL as the output data in the ANN model and inputting a series of training data into the ANN model system, the fitness functions of the targeted frequencies of 1000 Hz and 3000 Hz are established and shown below.

Table 1. The range and schedule levels of the parameters (case I).

Design parameters	Min [cm]	Max [cm]	4 Level [cm]			
L_{in}	0.0	6.0	0.0	2.0	4.0	6.0
L_1	4.5	9.0	4.5	6.0	7.5	9.0

Table 2. Sixteen training data sets (case I).

No. of experiment	L_{in} [cm]	L_1 [cm]
1	0	4.5
2	0	6.0
3	0	7.5
4	0	9.0
5	2	4.5
6	2	6.0
7	2	7.5
8	2	9.0
9	4	4.5
10	4	6.0
11	4	7.5
12	4	9.0
13	6	4.5
14	6	6.0
15	6	7.5
16	6	9.0

6.1.1. Target frequency – 1000 Hz

$$
\begin{aligned}
\mathrm{N1}_{1000} &= -1.29904 + 0.433013 \cdot L_1,\\
\mathrm{N2}_{1000} &= -3.89711 + 0.57735 \cdot L_{\text{in}},\\
\mathrm{N3}_{1000} &= -0.696222 + 1.21617 \cdot \mathrm{N1}_{1000}\\
&\quad + 0.742637 \cdot \mathrm{N1}_{1000}^2 - 0.769889 \cdot \mathrm{N1}_{1000}^3,\\
\mathrm{N4}_{1000} &= 0.592081 \cdot \mathrm{N2}_{1000} + \mathrm{N3}_{1000}\\
&\quad - 0.92679 \cdot \mathrm{N1}_{1000} \cdot \mathrm{N2}_{1000}\\
&\quad + 0.759725 \cdot \mathrm{N1}_{1000} \cdot \mathrm{N2}_{1000} \cdot \mathrm{N3}_{1000}\\
&\quad - 0.224864 \cdot \mathrm{N2}_{1000}^3,\\
\mathrm{TL}_{1000} &= 60.2717 + 6.22451 \cdot \mathrm{N4}_{1000}.
\end{aligned}
\tag{15}
$$

6.1.2. Target frequency – 3000 Hz

$$
\begin{aligned}
\mathrm{N1}_{3000} &= -1.29904 + 0.433013 \cdot L_1,\\
\mathrm{N2}_{3000} &= -3.89711 + 0.57735 \cdot L_{\text{in}},\\
\mathrm{N3}_{3000} &= -0.471739 \cdot \mathrm{N1}_{3000},\\
\mathrm{N4}_{3000} &= -1.54685 \cdot \mathrm{N3}_{3000}\\
&\quad - 2.0172 \cdot \mathrm{N1}_{3000} + 0.464778 \cdot \mathrm{N1}_{3000}^2\\
&\quad - 0.419782 \cdot \mathrm{N2}_{3000}^2\\
&\quad - 0.831301 \cdot \mathrm{N1}_{3000} \cdot \mathrm{N2}_{3000} \cdot \mathrm{N3}_{3000}\\
&\quad - 5.05405 \cdot \mathrm{N3}_{3000}^3 - 0.353539 \cdot \mathrm{N2}_{3000}^3,\\
\mathrm{N5}_{3000} &= -0.33531 + 0.718058 \cdot \mathrm{N4}_{3000}\\
&\quad + 0.538419 \cdot \mathrm{N4}_{3000}^2 + 0.230478 \cdot \mathrm{N4}_{3000}^3,\\
\mathrm{TL}_{3000} &= 40.78 + 12.22 \cdot \mathrm{N5}_{3000}.
\end{aligned}
\tag{16}
$$

6.2. Case II

Similarly, to optimize the acoustical performance within a limited space, two kinds of design parameters – L_1 and L – are chosen as the tuned variables. The range and schedule levels of the parameters are depicted in Table 3. Therefore, using the FEM run on the COMSOL package, the TL with respect to sixteen

Table 3. The range and schedule levels of the parameters (case II).

Design parameters	Min [cm]	Max [cm]	4 Level [cm]			
L_1	7.0	19.0	7.0	11.0	15.0	19.0
L	4.5	9.0	4.5	6.0	7.5	9.0

training data sets shown in Table 4 is calculated. Taking L_1 and L as the input data and the resulting TL as the output data in the ANN model and inputting a series of training data into the ANN model system, the fitness functions of the targeted frequencies of 1000 Hz and 3000 Hz are established and shown below.

Table 4. Sixteen training data sets (case II).

No. of experiment	L_{out1} [cm]	L_{out2} [cm]
1	7	4.5
2	7	6.0
3	7	7.5
4	7	9.0
5	11	4.5
6	11	6.0
7	11	7.5
8	11	9.0
9	15	4.5
10	15	6.0
11	15	7.5
12	15	9.0
13	19	4.5
14	19	6.0
15	19	7.5
16	19	9.0

6.2.1. Target frequency – 1000 Hz

$$\begin{aligned} \mathrm{N1}_{1000} &= -2.81458 + 0.216506 \cdot L_1, \\ \mathrm{N2}_{1000} &= -3.89711 + 0.57735 \cdot L, \\ \mathrm{N3}_{1000} &= 0.55662 \cdot \mathrm{N1}_{1000} \\ &\quad + 0.757491 \cdot \mathrm{N2}_{1000}, \\ \mathrm{TL}_{1000} &= 68.1207 + 7.36078 \cdot \mathrm{N3}_{1000}. \end{aligned} \tag{17}$$

6.2.2. Target frequency – 3000 Hz

$$\begin{aligned} \mathrm{N1}_{3000} &= -2.81458 + 0.216506 \cdot L_1, \\ \mathrm{N2}_{3000} &= -3.89711 + 0.57735 \cdot L, \\ \mathrm{N3}_{3000} &= 0.606632 - 0.316795 \cdot \mathrm{N1}_{3000} \\ &\quad - 1.80383 \cdot \mathrm{N2}_{3000} - 0.109147 \cdot \mathrm{N1}_{3000}^2 \\ &\quad - 0.537927 \cdot \mathrm{N2}_{3000}^2 + 0.293702 \cdot \mathrm{N1}_{3000}^3 \\ &\quad + 0.628958 \cdot \mathrm{N2}_{3000}^3, \\ \mathrm{TL}_{3000} &= 46.2844 + 11.1145 \cdot \mathrm{N3}_{3000}. \end{aligned} \tag{18}$$

7. Results and discussion

7.1. Results

7.1.1. Case I

By using the trained ANN model in conjunction with the GA optimizer, an optimized design at the targeted frequencies of 1000 Hz and 3000 Hz are obtained and shown in Tables 5 and 6. Plugging the original data and the optimal design data into COMSOL, the TL profiles before and after optimization is performed are plotted in Figs. 15 and 16. The range of GA's control parameters of *pop*, *bit*, $iter_{\max}$, *pc*, and *pm* are [40, 60, 80, 100], [5, 10, 20], [100, 200, 500, 1000], [0.2, 0.4, 0.6, 0.8], and [0.1, 0.3, 0.5, 0.7]. By varying the GA's control parameters step by step, the best GA set is obtained as (*pop*, *bit*, $iter_{\max}$, *pc*, *pm*) = (100, 20, 1000, 0.6, 0.5). As can be seen in Fig. 15, the TLs at the targeted frequency of 1000 Hz before and after performing an optimization are 33.96 dB and 67.87 dB. Similarly, as illustrated in Fig. 16, the TLs at the targeted frequency of 3000 Hz before and after performing an optimization are 47.57 dB and 59.96 dB. Moreover, because of the fixed diameters of the inlet tube, the

Table 5. The range and level of the design parameters (case I).

	L_{in} [cm]	L_1 [cm]
Original dimension	2.0	4.5
Optimal dimension (targeted tone: 1000 Hz)	0.5	8.9

Table 6. The range and level of the design parameters (case I).

	L_{in} [cm]	L_1 [cm]
Original dimension	2.0	4.5
Optimal dimension (targeted tone: 3000 Hz)	0.5	7.3

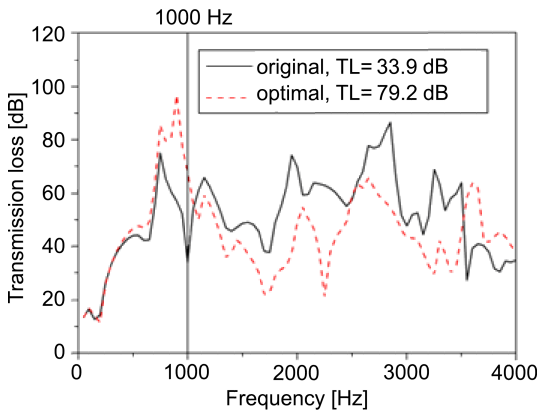

Fig. 15. TL before and after optimization at the targeted tone of 1000 Hz (case I).

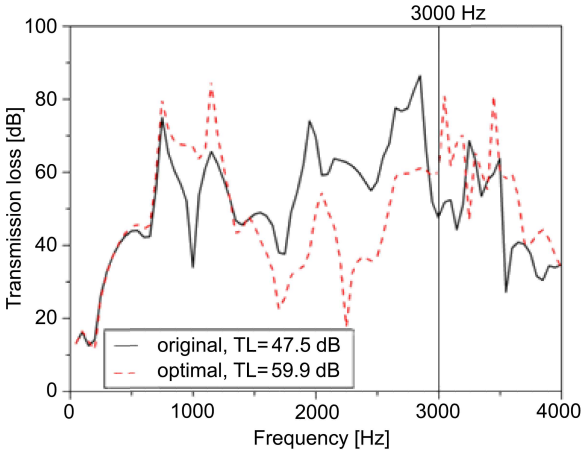

Fig. 16. TL before and after optimization at the targeted tone of 3000 Hz (case I).

internal tube, and the outlet tube, the flowing velocities remain the same. Using the back pressure formula shown in Eq. (6), the related back pressures of the muffler in the above simulation are calculated as 1331.6 Pa before and after the optimization.

The accuracy checks of the ANN model at the targeted frequencies of 1000 Hz and 3000 Hz have been verified by using the COMSOL package. The results for the targeted frequencies of 1000 Hz and 3000 Hz are depicted in Table 7 and Table 8, respectively. As indicated in Table 7, the accuracy of the ANN model at the targeted frequency of 1000 Hz reaches 3.22%. Likewise, as illustrated in Table 8, the accuracy of the ANN model at the targeted frequency of 3000 Hz reaches 2.7%.

Table 7. The accuracy check of the ANN model (case I).

	TL [dB]	Error [%]
Optimal TL(ANN) at 1000 Hz	70.1	3.22
Optimal TL(COMSOL) at 1000 Hz	67.9	
$\text{Error} = \frac{\text{TL(COMSOL)} - \text{TL(ANN)}}{\text{TL(ANN)}} \cdot 100\%$		

Table 8. The accuracy check of the ANN model (case I).

	TL [dB]	Error [%]
Optimal TL(ANN) at 3000 Hz	67.8	2.7
Optimal TL(COMSOL) at 3000 Hz	60.0	
$\text{Error} = \frac{\text{TL(COMSOL)} - \text{TL(ANN)}}{\text{TL(ANN)}} \cdot 100\%$		

7.1.2. Case II

By using the trained ANN model in conjunction with the GA optimizer, an optimized design at the targeted frequencies of 1000 Hz and 3000 Hz are obtained and shown in Tables 9 and 10. Plugging the original data and the optimal design data into COMSOL, the TL profiles before and after optimization is performed are plotted in Figs. 17 and 18. Similarly, by

Table 9. The range and level of the design parameters (case II).

	L_1 [mm]	L [mm]
Original dimension	13.4	4.5
Optimal dimension (targeted tone: 1000 Hz)	19.0	9.0

Table 10. The range and level of the design parameters (case II).

	L_1 [mm]	L [mm]
Original dimension	13.4	4.5
Optimal dimension (targeted tone: 3000 Hz)	10.7	5.5

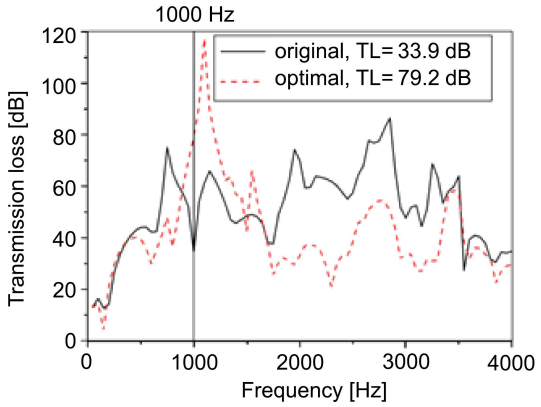

Fig. 17. TL before and after optimization at the targeted tone of 10 000 Hz (case II).

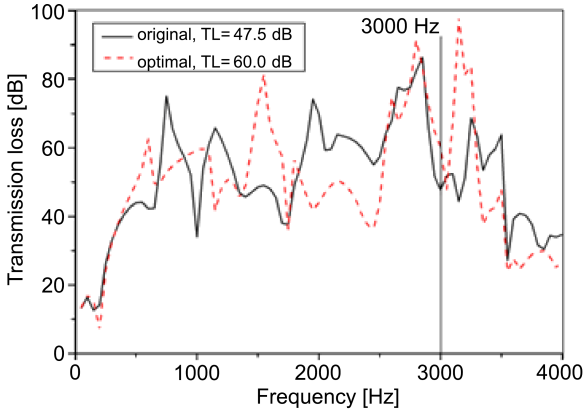

Fig. 18. TL before and after optimization at the targeted tone of 3000 Hz (case II).

varying the GA's control parameters step by step, the best GA set is obtained as (pop, bit, $iter_{\max}$, pc, pm) = (100, 20, 1000, 0.6, 0.5). As can be seen in Fig. 17, the TLs at the targeted frequency of 1000 Hz before and after performing an optimization are 33.96 dB and 79.26 dB. Similarly, as illustrated in Fig. 18, the TLs at the targeted frequency of 3000 Hz before and after performing an optimization are 47.57 dB and 60.06 dB. Furthermore, the related back pressures of the muffler in the above simulation remain 1331.6 Pa.

The accuracy checks of the ANN model at the targeted frequencies of 1000 Hz and 3000 Hz have been verified by using the COMSOL package. The results for the targeted frequencies of 1000 Hz and 3000 Hz are depicted in Tables 11 and 12, respectively. As indicated in Table 11, the accuracy of the ANN model at the targeted frequency of 1000 Hz reaches 1.69%. Likewise, as illustrated in Table 12, the accuracy of the ANN model at the targeted frequency of 3000 Hz reaches 4.38%.

Table 11. The accuracy check of the ANN model (case II).

	TL [dB]	Error [%]
Optimal TL(ANN) at 1000 Hz	80.6	1.69
Optimal TL(COMSOL) at 1000 Hz	79.3	
$\text{Error} = \frac{\text{TL(COMSOL)} - \text{TL(ANN)}}{\text{TL(ANN)}} \cdot 100\%$		

Table 12. The accuracy check of the ANN model (case II).

	TL [dB]	Error [%]
Optimal TL(ANN) at 3000 Hz	62.8	4.38
Optimal TL(COMSOL) at 3000 Hz	60.1	
$\text{Error} = \frac{\text{TL(COMSOL)} - \text{TL(ANN)}}{\text{TL(ANN)}} \cdot 100\%$		

7.2. Discussion

In order to simplify the numerical assessment of an automotive muffler with a complicated shape, a finite element model (FEM) used in predicting the muffler's TL is adopted. Moreover, to find an optimally shaped muffler, a simplified objective function (OBJ) with respect to the muffler at specified tones is established by linking the finite element model (FEM) with the artificial neural network (ANN) model.

As described in Sec. 3, the influence of the TL with respect to parameters D, L_1, L_{in}, and L shown in Figs. 6–9 is substantial. Here, the tendencies of TL and D are clear. TL will increase when D decreases. The other three parameters (L, L_1, and L_{in}) are closely related to the TL. However, the tendency for TL with respect to L_1, L_{in}, and L is uncertain. Therefore, L_1, L_{in}, and L are selected as the design parameters during the optimization process. Two kinds of parameter sets – (L_{in}, L) and (L_1, L) – are adopted in the optimization process. The numerical results of case I using the parameter set L_{in}, L are shown in Figs. 15 and 16. Results reveal that the optimized TLs are precisely located at the targeted frequencies of 1000 Hz and 3000 Hz. The noise reduction at the target tones of 1000 Hz and 3000 Hz can be improved by 33.91 dB and 12.39 dB after optimization is performed. Moreover, numerical results of case II using the parameter set L_{in}, L is shown in Figs. 17 and 18. Figures 17 and 18 indicate that the optimized TLs are also precisely located at the targeted frequencies of 1000 Hz and 3000 Hz. Similarly, the noise reduction at the targeted tones of 1000 Hz and 3000 Hz can be improved by 45.3 dB and 12.49 dB after optimization is performed. Furthermore, as indicated in Tables 7 and 8, case I's accuracy check of the ANN model and the FEM is between 2.7–3.22%. Case II's accuracy check of the ANN model and the FEM shown in Tables 11 and 12 is between 1.69–4.38%.Therefore, the assessment of an optimally shaped muffler in case I and case II is valid.

8. Conclusion

The traditional automobile muffler using a multi-chamber equipped with a straight resonating tube and a straight perforated tube in series will not only cause an increase in muffler length but also decrease the acoustical performance due to a straight venting path. In order to overcome these drawbacks, a multi-chamber muffler (hybridized with two internally parallel/extended tubes and one internally extended outlet) that has excellent noise reduction using a reverse path is presented. To design an optimal muffler within a space-constrained situation, the optimization of the muffler is also necessary. In addition, to reduce the noise transmission from the muffler's casing, a muffler's shell lined with a sound absorbing material is also adopted.

Sensitivity analysis reveals that the design parameters of D (diameter of the inlet tube in the first chamber), L_1 (length of the extended tube in the first chamber), L_{in} (length of the inlet tube for the second chamber), and L (length of the extended tube in the second chamber) are important in the shape optimization process. As can be seen in Sec. 2, the pressure drop of the muffler's interacting parts is closely related to both the geometric factors and the passing velocities. Based on the same geometric factors and the passing velocities of the fixed diameters of the internal

tubes, the muffler's pressure drop will remain the same during the optimization process. Also, the lengths of the tubes (L_1, L_{in}, and L) are selected as the design parameters.

To speed up the optimization for an automobile muffler that has a complicated shape, a simplified OBJ function using a FEM model (run on COMSOL) in conjunction with a neural network (ANN) model is built. After training and testing for the ANN model, the optimization process will be performed by linking the ANN model with the GA optimizer. Results reveal that in case I or case II, a muffler can be precisely optimized at targeted frequencies using the ANN model in concert with the GA method by adjusting the mufflers' shape under certain space constraints. As can be seen in the automobile muffler, it is one kind of reactive muffler. The muffler's TL curve will be shifted only when the optimization is performed by varying the lengths of the tubes. Prospectively, the primary peak of the TL curve will be adjusted to the desired frequency; however, the TLs at other frequencies will possibly be decreased.

Consequently, this paper provides a quick way to design an optimally shaped hybrid muffler that has a compact mechanism and an improved acoustical performance for an automotive venting system.

Acknowledgments

The authors acknowledge the financial support of Ministry of Science and Technology (MOST 104-2221-E-036-027, ROC).

References

1. Bies D.A., Hansen C.H. (1988), *Engineering noise control*, Unwin Hyman, New York.

2. Chang Y.C., Chiu M.C., Cheng M.M. (2009), *Optimum design of perforated plug mufflers using neural network and genetic algorithm*, Proceedings of the Institution of Mechanical Engineers, Part C: Journal of Mechanical Engineering Science, **223**, 4, 935–952.

3. Chang Y.C., Yeh L.J., Chiu M.C. (2004), *Numerical studies on constrained venting system with side inlet/outlet mufflers by GA optimization*, Acta Acustica united with Acustica, **90**, 6, 1159–1169.

4. Chen J., Shi X. (2011), *CFD numerical simulation of exhaust muffler*, 2011 Seventh International Conference on Computational Intelligence and Security, pp. 1438–1441.

5. Chiu M.C. (2013), *Shape optimization of multi-chamber tube-extended mufflers within specified back pressures using a particle swarm method*, Noise & Vibration Worldwide, **44**, 3, 10–23.

6. Chiu M.C., Chang Y.C. (2009), *Application of neural network and genetic algorithm to the optimum design of perforated tube mufflers*, Journal of Mechanics, **25**, 3, N7–N16.

7. Chiu M.C., Chang Y.C., Huang C.L., Cheng H.C. (2016), *Venting noise abatement using a cylindrical dissipative muffler and genetic method*, Sylwan Journal, **160**, 3, 271–299.

8. Fang J., Zhou Y., Jiao P., Ling Z. (2009), *Study on pressure loss for a muffler based on CFD and experiment*, 2009 International Conference on Measuring Technology and Mechatronics Automation ICMTMA'09, Vol. 3, pp. 887–890.

9. Galphade A., Patil A.V. (2015), *Design and analysis of muffler for 800 cc car*, International Journal of Advance Research in Engineering, Science & Technology, **2**, 7, 72–76.

10. Holland J. (1975), *Adaptation in natural and artificial system*, Ann Arbor: University of Michigan Press.

11. Ih J.G. (1992), *The reactive attenuation of rectangular plenum chambers*, Journal of Sound and Vibration, **157**, 1, 93–122.

12. Ivakhnenko A.G. (1971), *Polynomial theory of complex system*, IEEE transactions on Systems, Man, and Cybernetics, **1**, 4, 364-368.

13. Jong D. (1975), *An analysis of the behavior of a class of genetic adaptive systems*, Doctoral thesis, Dept. Computer and Communication Sciences, Ann Arbor, University of Michigan.

14. Kore S., Aman A., Direbsa E. (2011), *Performance evaluation of a reactive muffler using CFD*, Journal of EEA, **28**, 83–89.

15. Lyu B.H. (2005), *An Investigation in design and performance of reactive muffler for dry pump*, Master degree, Chung Yuan Christian University.

16. Mo J.Y., Huh M.S. (1994), *A study on the analysis and improvement of the acoustic characteristics of the muffler with complex geometry*, International Compressor Engineering Conference.

17. Mohiuddin A.K.M., Rahman Ataur, Gazali Y.B. (2007), *Simulation and experimental investigation of muffler performance*, International Journal of Mechanical and Materials Engineering (IJMME), **2**, 2, 118–124.

18. Panigrahi S.N., Munjal M.L. (2007), *Backpressure considerations in designing of cross flow perforated-element reactive silencer*, Noise Control Engineering Journal, **55**, 6, 504–515.

19. Patrikar A., Provence J. (1996), *Nonlinear system identification and adaptive control using polynomial networks*, Mathematical and Computer Modelling, **23**, 1/2, 159–173.

20. Potente D. (2005), *General design principles for an automotive muffler*, Proceedings of Acoustics, pp. 153–158.

21. Rajadurai S., Ananth S. (2014), *Muffler development for diesel hybrid vehicle*, International Journal of Innovative Science, Engineering & Technology, **1**, 9, 513–519.

22. Reddy M.R., Reddy K.M. (2012), *Design and optimization of exhaust muffler in automobiles*, International Journal of Engineering Research and Applications, **2**, 5, 395–398.

23. Somashekar G., Prakasha A.M., Ahamd N., Badrinarayan K.S. (2015), *Modal analysis of muffler of an automobile by experimental and numerical approach*, International Journal of Recent Research in Civil and Mechanical Engineering, **2**, 1, 309–314.

24. Tajane A., Jadhav M., Rathod R., Elavande V. (2014), *Design and testing of automobile exhaust system*, International Journal of Research in Engineering and Technology, **3**, 11, 164–168.

25. Vasile O., Gillich G. (2012), *Finite element analysis of acoustic pressure levels and transmission loss of a muffler*, [in:] *Advances in Remote Sensing, Finite Differences and Information Security*, Scutelnicu E., Lazic L., de Arroyabe P.F. [Eds.], Wseas LLC, pp. 43–48.

26. Yeh L.J., Chang Y.C., Chiu M.C. (2006), *Numerical studies on constrained venting system with reactive mufflers by GA optimization*, International Journal for Numerical Methods in Engineering, **65**, 8, 1165–1185.